Modulation by geraniol of gene expression involved in lipid metabolism leading to a reduction of serum-cholesterol and triglyceride levels

Marianela Galle , Boris Rodenak Kladniew , María Agustina Castro , Sandra Montero Villegas , Ezequiel Lacunza , Mónica Polo , Margarita García de Bravo , Rosana Crespo

PII: S0944-7113(15)00111-7
DOI: 10.1016/j.phymed.2015.04.005
Reference: PHYMED 51823

To appear in: *Phytomedicine*

Received date: 24 December 2014
Revised date: 18 April 2015
Accepted date: 24 April 2015

Please cite this article as: Marianela Galle , Boris Rodenak Kladniew , María Agustina Castro , Sandra Montero Villegas , Ezequiel Lacunza , Mónica Polo , Margarita García de Bravo , Rosana Crespo , Modulation by geraniol of gene expression involved in lipid metabolism leading to a reduction of serum-cholesterol and triglyceride levels, *Phytomedicine* (2015), doi: 10.1016/j.phymed.2015.04.005

Modulation by geraniol of gene expression involved in lipid metabolism leading to a reduction of serum-cholesterol and triglyceride levels

Marianela Galle[a], Boris Rodenak Kladniew[a], María Agustina Castro[a], Sandra Montero Villegas[a], Ezequiel Lacunza[b], Mónica Polo[a], Margarita García de Bravo[a] and Rosana Crespo[a,*]

[a]INIBIOLP (UNLP-CONICET CCT La Plata), Facultad de Ciencias Médicas. Calles 60 y 120, La Plata, Argentina

[b]CINIBA (UNLP-CONICET CCT La Plata), Fac. de Ciencias Médicas. Calles 60 y 120, La Plata, Argentina

**Corresponding author:*
Present address: INIBIOLP (CONICET, CCT La Plata – UNLP). Facultad de Cs. Médicas. Calles 60 y 120, La Plata, Argentina. Tel.: +54 221 4824894; fax: +54 221 4258988. E-mail address: rcrespo@med.unlp.edu.ar

Abstract

Background: Geraniol (G) is a natural isoprenoid present in the essential oils of several aromatic plants, with various biochemical and pharmacologic properties. Nevertheless, the mechanisms of action of geraniol on cellular metabolism are largely unknown.

Hypothesis/Purpose: We propose that geraniol could be a potential agent for the treatment of hyperlipidemia that could contribute to the prevention of cardiovascular disease. The aim of the present study was to advance our understanding of its mechanism of action on cholesterol and TG metabolism.

Study Design/Methods

NIH mice received supplemented diets containing 25, 50, and 75 mmol G/kg chow. After a 3-week treatment, serum total-cholesterol and triglyceride levels were measured by commercial kits and lipid biosynthesis determined by the [14C] acetate incorporated into fatty acids plus nonsaponifiable and total hepatic lipids of the mice. The activity of the mRNA encoding HMGCR—the rate-limiting step in cholesterol biosynthesis—along with the enzyme levels and catalysis were assessed by real-time RT-PCR, Western blotting, and HMG-CoA-conversion assays, respectively. In-silico analysis of several genes involved in lipid metabolism and regulated by geraniol in cultured cells was also performed. Finally, the mRNA levels encoded by the genes for the low-density-lipoprotein receptor (LDLR), the sterol-regulatory-element-binding transcription factor (SREBF2), the very-low-density-lipoprotein receptor (VLDLR), and the acetyl-CoA carboxylase (ACACA) were determined by real-time RT-PCR.

Results: Plasma total-cholesterol and triglyceride levels plus hepatic fatty-acid, total-lipid, and nonsaponifiable-lipid biosynthesis were significantly reduced by geraniol feeding. Even though an up-regulation of the mRNA encoding HMGCR occurred in the geraniol-treated mouse livers, the protein levels and specific activity of the enzyme were both inhibited. Geraniol also enhanced the mRNAs encoding the LDL and VLDL receptors and reduced ACACA mRNA, without altering the transcription of the mRNA encoding the SREBF2.

Conclusions: The following mechanisms may have mediated the decrease in plasma lipids levels in mice: a down-regulation of hepatocyte-cholesterol synthesis occurred as a result of decreased HMGCR protein levels and catalytic activity; the levels of LDLR mRNA became elevated, thus suggesting an increase in the uptake of serum LDL, especially by the liver; and TG synthesis became reduced very likely because of a decrease in fatty-acid synthesis.

Keywords: Geraniol, Hypolipemia, Lipogenesis, HMGCR, ACACA

Abbreviation:

ACACA: acetyl-CoA carboxylase

G: Geraniol

HMG-CoA: 3-hydroxy-3-methylglutarylcoenzyme-A

HMGCR: 3-hydroxy-3-methylglutarylcoenzyme-A reductase

LDL: low-density-lipoprotein

LDLR: low-density-lipoprotein receptor

MP: mevalonate pathway

RT-PCR: reverse-transcriptase–polymerase-chain reaction

SREBF2: sterol-regulatory-element–binding transcription factor

TG: triglyceride

VLDL: very-low-density-lipoprotein

VLDLR: very-low-density-lipoprotein receptor

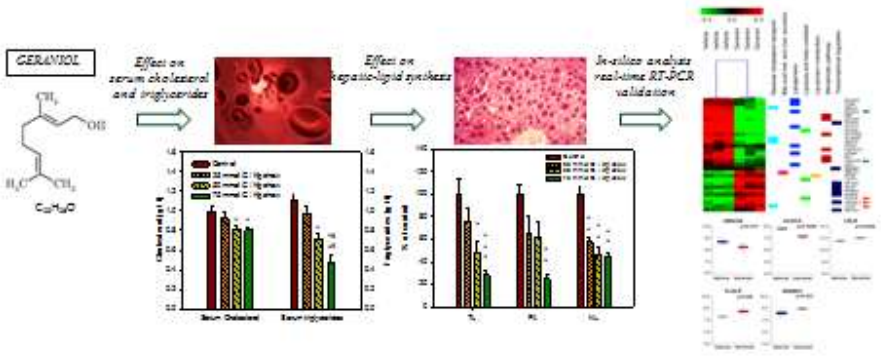

1. Introduction

Geraniol (G) is an acyclic monoterpene derived from the mevalonate pathway (MP) in plants, but not produced in mammals. This natural isoprenoid—present in the essential oils of diverse aromatic plants—is produced by the flowers but is present in the vegetative tissues from species of the Rosaceae, Poaceae, Lamiaceae, Geraniaceae, Rutaceae families. Because of its organoleptic features, geraniol is one of the most frequently used compound in the fragrances and flavoring industries (Chen and Viljoen, 2010; Lapczynski et al., 2008). This terpenoid has previously shown antiproliferative activity against human tumor cells both in culture and *in vivo* (Ahmad et al., 2011; Burke et al., 1997; Cardozo et al., 2011; Carnesecchi et al., 2001; Galle et al., 2014; Jin et al., 2013; Ong et al., 2006). G appears to decrease tumor growth by cell-cycle arrest, apoptosis induction, and autophagy (Cardozo et al., 2011; Chaudhary, et al., 2013; Kim et al., 2012; Ong et al., 2006; Wiseman et al., 2007). Nevertheless, the mechanisms of action of geraniol on cellular metabolism are largely unknown. The MP has been reported as a metabolic sequence modulated by isoprenoids (Mo and Elson, 2004; Ong et al., 2006). In addition to cholesterol, the pathway generates several other molecules relevant to general cellular metabolism, such as farnesyl pyrophosphate and geranyl-geranyl pyrophosphate, essential in the prenylation of a variety of proteins including the small GTPase Ras, which plays a critical role in cell-cycle progression. The rate-limiting enzyme of the MP is 3-hydroxy-3-methylglutarylcoenzyme-A reductase (HMGCR), a protein that is transcriptionally regulated by the sterol-regulatory-element–binding transcription factor (SREBF2).

Our recently published work (Galle et al., 2014) performed in a mouse model in which geraniol exerted antitumor activity as well as caused the inhibition of the MP, also demonstrated a reduction of plasma cholesterol and triglyceride (TG) levels in tumor-bearing host mice. Whether the hypolipidemic effect was caused by an increase in the tumor's lipid requirements for growth or by the presence of geraniol itself, however, remained unclear. The aim of the present study was to

advance our understanding of the mechanism of action of this monoterpene on cholesterol and TG metabolism in non–tumor-bearing mice. For this purpose we evaluated the plasma-lipid content, the lipid-biosynthetic levels, and the genetic expression of certain key proteins involved in the regulation of those lipid levels that had been previously found to be modified with geraniol in cultured cells and *in vivo* (Crespo et al., 2013; Galle et al., 2014; Jayachandran et al., 2014): namely, HMGCR, -acetyl-CoA carboxylase (ACACA, catalyzing the rate-limiting step in fatty-acid biosynthesis), SREBF2, the low-density-lipoprotein (LDL) receptor, (mediating LDL-cholesterol internalization into the cell), and the very-low-density-lipoprotein (VLDL) receptor—it apparently playing an essential role in the uptake and degradation of fatty acids and TG-rich particles (Crawford et al., 2008).

2. **Materials and methods**

2.1 Reagents

Geraniol (98%) was obtained from Sigma (St. Louis, MO, USA), inorganic reagents and solvents of analytical grade from Merck (Darmstadt, Germany), analyticals from Carlo Erba (Milan, Italy) and Sigma, and [^{14}C] acetate (54.7 Ci/mol) from Perkin Elmer Life Science, Inc. (Boston, MA, USA). Merck, Sharp and Dohme (Argentina) kindly provided simvastatin.

2.2 Animals and diets

Female NIH *nu/nu* mice were obtained from the Bioterio of Centro Atómico Ezeiza (CNEA) and housed in a temperature-controlled room on a 12/12-h cycle of light and darkness. The animals were maintained *ad libitum* on a gamma-irradiated-chow diet and autoclaved water. Two-month-old mice with 20–25g weight were randomly separated into one control group and three experimental groups, with the latter receiving supplemented diets containing 25, 50, and 75 mmol G/kg chow as described in previous reports (Yu et al., 1995; Galle et al., 2014). A positive control for hypolipidemic effects was included; this group was treated with 50 mg/kg body

weight of simvastatin per day in the drinking water. After a 3-week treatment, all mice were injected with radioactive acetate (25 μCi/animal) and three h later killed by cervical dislocation in the middle of the light period. All experiments on animals were performed in conformity with *Guidelines of Handling and Training of Laboratory Animal* (Wolfensohn and Lloyd, 2013). The animal-use protocols employed were approved by the Institutional Animal Care and Use Committee (IACUC), Facultad de Ciencias Médicas, Universidad Nacional de La Plata. Protocol number 04-001-13.

2.3 Blood measurements

Samples—removed from serum prepared from mouse blood obtained by cardiac puncture at sacrifice—were placed at 37 °C for 30 min, centrifuged for 10 min at 3000 x *g*, and then stored at –20 °C until analysis. Cholesterol and TG concentrations were determined by commercial kits (Wiener, Argentina) adapted to use with mice. The samples were incubated at 37 °C for 5 min and the A^{505} measured within 30 min in a Beckman Coulter DTX 880 Microplate Reader. A standard curve of A_{505}*vs*.cholesterol or TG concentration was plotted and the total concentrations in the sample calculated from the standard curve.

2.4 Tissue collection and histological analysis

Whole livers were removed from the mice and the total-liver weights measured. Fresh-liver blocks were cut and immediately fixed in 10% (v/v) buffered formaldehyde, then dehydrated in graded alcohols and embedded in paraffin. Sections of 6-μm thickness were rehydrated and stained with hematoxylin-eosin and the stained sections observed under light microscopy.

2.5 Liver- lipid extraction and analysis

Liver lipids were extracted with chloroform:methanol (2:1, v:v) (Folch, Lees, & Sloane Stanley, 1957). In one aliquot from the organic phase, the TGs and the free

and esterified cholesterol were separated by thin-layer chromatography on silica gel geraniol developed in hexane/diethylether/acetic acid 80/20/1 (v/v/v), revealed through the use of a spray reagent containing an acidic ferric-chloride solution (Dudley & Anderson, 1975; Ren and Gould, 1994; Wilson and Sargent, 1992), and finally quantified by means of a curve constructed with pure standards (free cholesterol, esterified cholesterol, and trimiristine) that had been run on the same plate. The spots' images were analyzed by the Image J program. Another aliquot was used for measuring the radioactivity incorporated into total liver lipids and into the nonsaponifiable fraction plus the fatty acids resulting from a previous saponification reaction with 10% (w/v) KOH in methanol at 85 °C for 45 min. The nonsaponifiable lipids were extracted with petroleum ether, while after acidification the fatty acids were further extracted from the aqueous phase with petroleum ether.

The radioactivity was measured in a Wallac 1214 Rackbeta liquid-scintillation counter (Pharmacia, Turku, Finland).

2.6 RNA isolation and analysis by the real-time reverse-transcriptase–polymerase-chain reaction

Total RNA was extracted from mouse liver through the use of the TRI Reagent (Molecular Research Center, Inc., Cincinnati, OH, USA) followed by a DNAase-I treatment (Fermentas Life Sciences, city, country). The cDNA was then synthesized by means of the kit qScriptTM cDNA SuperMix (Quanta Bioscences, Inc., city, country). The analysis by the real-time reverse-transcriptase–polymerase-chain reaction (real-time RT-PCR) was run through the use of the PerfeCtaTM SyberGreenFastMixTM and the StratageneMX30005P real-time–RT-PCR System. The PCR conditions were 94 °C for 4 min, followed first by 40 cycles with each one under the following conditions: 94 °C for 40 s, 57 °C for 40 s, and 72 °C for 40 s; and then by a final cycle at 95 °C for 1 min, 55 °C for 30 s, and 95 °C for 30 s. The relative amount of mRNA was calculated by means of the comparative-threshold-cycle method and the qBase v1.3.5 program with ß-actin as the reference

housekeeping gene. The oligonucleotide primers used are summarized in Table 1. The amplified fragments were detected by electrophoresis on a 1.8% (w/v) agarose gels after Sybr-Green-I staining.

2.7 HMGCR in the microsomal fraction

Mouse-liver tissue was placed (1:10, w/v) in cold homogenization buffer containing 0.3 M sucrose, 50 mM NaCl, 10 mM sodium ethylenediaminetetracetic acid, 10 mM dithiothreitol, and 50 mM Tris-HCl (pH 7.4). The minced tissue was homogenized at 4 °C in a TRI–R 5630 homogenizer [commercial source]. Samples were centrifuged at 12,000 x *g* and 4 °C for 15 min and the resulting supernatant fraction at 105,000 x *g* and 4 °C for 60 min. The final microsomal pellets were immediately frozen at –70 °C for storage until use. Before the assay for HMGCR activity, each pellet was resuspended in buffer containing 5 mM dithiothreitol and 20 mM imidazole chloride (pH 7.4). The protein content of each sample was determined by the method of Bradford (1976) with bovine-serum albumin as standard.

The spectrophotometric assay of the solubilized HMGCR containing 0.2 mM NADPH and 0.1 mM RS-HMG-CoA in phosphate buffer (0.2 M KCl, 0.16 M potassium phosphate, 0.004 M ethylenediaminetetracetic acid, and 0.01 M dithiothreitol, pH 6.8) was carried out at 37 °C through the use of a Beckman Coulter DTX 880 Microplate Reader. One unit of HMGCR activity was defined as 1 pmol of NADPH consumed per min per mg microsomal protein.

For Western blotting, microsomal proteins were boiled in the sample buffer (Tris-HCl 0.06M pH 6.8, Glycerol 1%, Bromophenol blue 0.02%, SDS 2%, ß-mercaptoethanol5%) for 5 min. The samples were separated on 12.5% (w/v) sodium-dodecylsulfate–polyacrylamide gels and adsorbed to polyvinylidenedifluoride membranes (Amersham, GE Healthcare,[commercial source]) by a semidry transfer at 10 V for 1 h in 20% (v/v) methanol in 39 mM glycine, 48 mM Tris pH 8.3. The nonspecific protein-binding sites were blocked by

incubation in PBS (pH 7.4) containing 0.05% (v/v) Tween 20 plus 5% (v/v) skimmed milk. The membrane was incubated with anti-HMGCR (Santa Cruz, CA, USA) diluted 1/200 in antibody-dilution buffer (2% [v/v] skimmed milk in PBS plus 0.1% [v/v] Tween 20) for 1 h followed by three 5-min washes in the same buffer. Horseradish-peroxidase–conjugated antibodies (Santa Cruz, CA, USA) were added to the membrane for 1 h. As an internal control, polyvinylidenedifluoride membranes were stained with Coomassie blue G-250.

Immunoreactive bands were detected by enhanced-chemiluminescence Western-blot–detection reagents (Amersham Pharmacia Biotech, city, country) and processed manually through the use of common X-ray-film developers and fixers. Protein immunoblots were scanned and the density of each band quantified with the ImageJ software (Image processing and analysis in Java).

2.8 In-silico *analysis*

The effect of geraniol on the gene-expression profiles of loci associated with lipid metabolism was assessed *in silico*. We employed the dataset GSE45567 obtained from GEO (http://www.ncbi.nlm.nih.gov/geo/), in which several compounds, including geraniol, were evaluated in triplicate on the PC-3 permanent cell-culture line (Lee et al., 2013). These cells—originally derived from a human-prostate cancer and containing prostasome membranes enriched in lipid rafts of cholesterol and sphingomyelin (Llorente et al., 2007)—synthesize and accumulate more cholesterol than normal prostate epithelial cells (Li et al., 2006). The relevant data were downloaded as .CEL files and normalized with the frozen robust multiarray-analysis (fRMA) algorithm in the open-source statistical software R. From the normalized matrix obtained, the vehicle- and geraniol-treated samples were extracted and compared statistically. A total of 64 genes—grouped into 7 functional categories—were analyzed (Supplementary material).

We applied the unsupervised-hierarchical-clustering method by means of the MeV software (www.tm4.org/mev.html) with the Pearson correlation coefficient as a measurement of distance and complete linkage.

2.9 Statistical analysis

The results are expressed as the means ± S.E.M., and all analyses were conducted with GraphPadInStat 3.0. Statistical differences between the control and the geraniol-treated animals were evaluated by the ANOVA test followed by the Tukey HSD *post-hoc* comparisons. Differences were considered significant at a $p < 0.05$. For the *in-silico* analysis, the differences in the gene-expression profiles between the samples exposed to the vehicle and those treated with geraniol were evaluated by the TTest (Dudoit et al., 2002; Pan, 2002) at a significance threshold of 0.05% (Supplementary material).

3. **Results**

3.1 Serum-cholesterol and -TG levels after geraniol treatment

Mice treated with 25, 50, and 75 mmol G/kg chow manifested a decrease in serum cholesterol and TGs (Fig. 1), and this effect became significant ($p < 0.05$) in the mice treated with 50 and 75 mmol G/kg chow. Moreover, in mice fed with the highest dose of geraniol, the reduction in serum-TG content compared to the controls was much more pronounced than that of the cholesterol (by 58.2% and 18.7%, respectively). The effect of simvastatin (50 mg/kg), as a standard hypolipidemic drug, was similar to that obtained with the lowest dose of geraniol (Fig. 1). In order to compare geraniol with simvastatin, geraniol impregnated into the chow was quantified by capillary gas chromatography (data not shown), which determination suggested that 25, 50, and 75 mmol geraniol added per kg of the chow, would result in 100, 200, and 300 mg G/kg body weight of each animal per day, respectively.

The decrease in these blood lipids seemed not to produce any adverse side

effects in the mice since after the 3-week experimental period the final body and liver weights, as well as the levels of food intake, in the treated mice were not significantly different from the corresponding values in the control mice (Table 2). This outcome contrasts with what is commonly observed in animals subjected to toxic compounds (Wang et al., 2007). Moreover, the general histologic organization of the livers of the G-fed mice was similar to that of the control mice: none of the animals manifested hepatic steatosis, an accumulation of pigments, a congestion of the hepatic vessels, or the presence of macrophages and lymphocyte infiltrates (Fig. 2 A-D).

3.2 Liver-lipid profile and lipid synthesis of mice treated with geraniol

In contrast to the results with serum, when the content of TGs and of free and esterified cholesterol were analyzed in the livers of geraniol-treated mice, no significant differences were found in any of those lipid classes with respect to the control values (Fig. 3A, B).

When the incorporation of [^{14}C]acetate into total lipids, fatty acids, and nonsaponifiable lipids was investigated, low doses of geraniol (25 mmol/kg chow) did not significantly decrease the radiolabelling in the total lipids, but at 50 or 75 mmol G/kg chow, a diminution in incorporation became progressively significant. Fatty-acid synthesis was significantly inhibited only at the highest dose of geraniol, whereas nonsaponifiable-lipid synthesis was substantially reduced at all three doses of the isoprenoid (Fig. 4).

3.3 In silico *analysis of the effect of geraniol on lipid metabolism and the expression of related genes in PC-3 cells*

Hierarchical clustering revealed two stable groups, the vehicle-exposed (a working solution of 0.01% [v/v] ethanol) and the geraniol-treated cells. Similarly, at the genetic level two stable clusters were identified from the first node of the dendogram. We designated these clusters as being up-regulated or down-regulated

upon treatment with geraniol. That the genes related to lipogenesis all segregated into the down-regulated cluster, whereas those involved in lipoprotein metabolism all seemed to be activated by geraniol treatment was most interesting. The distribution of genes from the other functional categories varied between the two clusters: The genes encoding bile-acid metabolism and cholesterol excretion showed a tendency to be activated, with 6 genes in the up-regulated *versus* 3 in the down-regulated cluster (at 66% overall); the genes related to cholesterol transport exhibited the reverse pattern, with 3 out of 4 in the down-regulated cluster (at 75% overall); the genes responsible for lipolysis and ß-oxidation were principally up-regulated, with 5 out of 7 in that cluster (at 71% overall); and finally the genes governing the MP proved to be essentially divided, with 13 out of 20 in the down-regulated cluster (65% overall; Fig. 5A).

TTest analysis for these genes between the vehicle-exposed and the geraniol-treated cells—at a significance level of 0.05—indicated that ACSL1, ABCA1, DHCR24, ACAT2, ACACA, ABCG1, ACAD9, ACACB, IDI1, PPARG, SCD, SCARB1, HMGCS1, EBP, DHCR7, FASN, HMGCR, and GPAM were down-regulated upon G treatment; whereas NR1H2, PPARA, INSIG2, CPTP1, APOE, VLDLR, ABCC2, and SREBF2 were activated after exposure to geraniol (Fig. 5, Panel B). Furthermore, the reverse cholesterol transport, lipogenesis, and MP biofunctions were down-regulated. On the basis of these results and the previous data from our own laboratory, we decided to validate five of these genes (HMGCR, ACACA, LDLR, VLDLR, and SREBF2) in the livers of geraniol-treated mice, as this organ plays a major role in cholesterol and lipid metabolism (van der Wulp et al., 2013).

3.4 Effect of geraniol on the HMGCR of mouse liver

The analysis of HMGCR expression by real-time RT-PCR revealed a dose-dependent increase in the mount of the mRNA encoding the enzyme. The highest dose of geraniol (75 mmol G/kg chow) produced a statistically significant rise in the

mRNA levels in the livers of the mice compared to the control values (Fig. 6, Panel A). Nevertheless, the levels and specific activities of the protein in the microsomes decreased reciprocally with increases in the doses of G (Fig. 6, panels B and C), resulting in a statistically significant effect on each of the two parameters at respective doses of 75 and 50 plus 75 mmol G/kg chow.

3.5 Effect of geraniol on the LDL-receptor–, ACACA-, VLDL-receptor–, and SREBF2-mRNA transcription

In order to evaluate cholesterol uptake by the liver, we measured the transcriptional expression of the LDL receptor. As determined by real-time RT-PCR, the LDL receptor mRNA was significantly increased in mice fed with 50 and 75 mmol G/kg chow (Fig. 7A). The SREBF2-mRNA levels, however, did not vary significantly under either feeding condition (Fig. 7, Panel B). To ascertain the possible reason for the decrease in serum TG, we evaluated the mRNA levels of ACACA, the rate limiting enzyme in the fatty-acid synthesis. We observed that geraniol tended to inhibit ACACA transcription in animals treated with the middle dose, with this inhibition becoming statistically significant at 75 mmol G/kg chow (Fig. 8A). Moreover, by measuring the VLDL-receptor mRNA we also were able to evaluate the TG removed from VLDL by liver cells. These results indicated that the VLDL-receptor expression was up-regulated by geraniol (Fig. 8B). This increased transcription was statistically significant in mice fed with 50 mmol G/kg chow. Finally, most of these determinations of gene expression by real-time RT-PCR were consistent with the analyses *in silico* illustrated in Fig. 5.

4. **Discussion**

In the present work we have demonstrated that geraniol, a natural monoterpene present in the essential oils of several plants, significantly diminished the triglyceride and cholesterol levels in mouse blood, without exerting any effect on the animals' gain in body weight, food intake (Table 2), or liver histology (Fig. 2).

Furthermore, mice fed with 50 and 75 mmol G/kg of the diet exhibited a reduction in the synthesis of total liver lipids, especially with respect to the nonsaponifiable fraction (Fig. 4), where cholesterol biosynthesis was presumably the main process inhibited by geraniol, as we had demonstrated in several previous studies on cultured cells (Crespo et al., 2013; Polo et al., 2011; Polo et al., 2006). These results encouraged us to consider geraniol as a phytochemical with potential as an agent for combatting hypercholesterolemia. Since 50% or more of the total cholesterol in humans derives from *de-novo* synthesis, one of the most effective means to reduce the sterol's levels is undoubtedly an inhibition of its endogenous synthesis at the hepatic level (Vallianou et al., 2011). We suggest that HMGCR inhibition would be one of the multiple effects that isoprenoid compounds seem to be exerting on the MP, though that possibility had not yet been specifically elucidated previously. Only few citations in the literature (Duncan et al., 2004; Peffley and Gayen, 2003)—in addition to previous studies from our laboratory (Crespo et al., 2013) and the data obtained from the *in-silico* analysis presented here—have documented both a transcriptional and a posttranscriptional inhibition of the enzyme in cultured tumor cells. Our *in-vivo* results are in accord with the aforementioned reports on cultured cells since the animals treated with geraniol evidenced a decrease in both the levels and the activity of hepatic HMGCR even though the enzyme-specific mRNA levels increased in a dose-dependent manner (Fig. 6).

Regarding the regulation of HMGCR messenger levels, despite the indication by *in-silico* analysis that SREBF2 mRNA—which transcript modulates the expression of the HMGCR structural gene—was overexpressed in cultured geraniol-treated cells, our work demonstrated that those regulatory-mRNA levels did not vary in the livers of mice treated with geraniol (Fig. 7); possibly because, in addition to affecting the SREBF2 gene's expression at the transcriptional level, the monoterpene could be regulating, directly or indirectly, the maturity mechanism of this transcription factor—involving a cleavage in the endoplasmatic reticulum and thus a prevention of nuclear migration—in agreement with the reports of Espenshade &

Hughes (2007) and Sato (2009).

In order to gain a more complete understanding of the role of SREBF2 transcription in the modulation of cholesterol levels under these experimental conditions, we also evaluated the effect of geraniol on LDL-receptor mRNA—its gene constituting another target of the mature SREBF2 mRNA (Sato, 2009)—since one of the mechanisms that participates in cellular-cholesterol homeostasis is the uptake of cholesterol from the serum mainly through the internalization of LDL-cholesterol via the LDL receptor (Chang et al., 2006) within the LDL pathway (Goldstein and Brown, 1990). The increase in LDL-receptor mRNA in mice treated with all three geraniol doses was only statistically significant from the second dose assayed, which response correlated with the diminution observed in serum-cholesterol levels (Fig. 7, Panel A and Fig. 1, respectively). These results, together with the observation that the cholesterol levels in liver were not modified by the treatments with geraniol (Fig. 3), suggest the occurrence of an overexpression of the LDL-receptor gene to produce an increased uptake of exogenous cholesterol as a compensatory mechanism to offset the decrease in endogenous cholesterogenesis.

Geraniol also produced a decline in serum TG (Fig. 1). Moreover, the decreases in the incorporation of [^{14}C]acetate into fatty acids in the livers of the treated mice (Fig. 4) along with the drop in the ACACA-mRNA levels (Fig. 8) support the hypothesis that the lowering of the serum TG concentration effected by geraniol could have been mediated by that concomitant inhibition of the synthesis of fatty acids. Nevertheless, serum TG significantly decreased with doses of geraniol that did not yet produce a statistically significant inhibition in fatty-acid synthesis (*cf*. Figs. 1 and 4). Consequently, we consider that other regulatory mechanisms involved in the metabolism of fatty acids could be operating to produce the lowering of serum TG. Since VLDL transports TG in the serum and the VLDL receptor has been proposed to bind VLDL as well as lipoprotein lipase and thus facilitate lipolysis (Crawford et al., 2008; Tacken et al., 2000)—or even to induce VLDL uptake (Guo-Min et al., 2012)—the overexpression of the VLDL-receptor gene

induced by G (Fig. 8) should be associated with an elevated removal of TG from the serum. Furthermore, similar hypolipidemic effects and molecular mechanisms have been shown in mice treated with the essential oils from *Melissa officinalis* (Jun et al., 2014). Accordingly, on the basis of the *in-silico* analyses presented here, we hypothesized that geraniol induced a fundamental change in the expression of several key genes involved in lipid metabolism resulting in a significant decrease in lipogenic-gene expression, particularly those related to the synthesis of cholesterol, fatty acids, and the saponifiable lipids; all of those gene products being targets for SREBF2 and SREBF1c. Furthermore, SREBF1c expression was down-regulated and nuclear-receptor-gene expression also modified by geraniol (*cf.* Fig. 5): there the peroxisome proliferator-activated receptor-(PPARA) and the farnesoid X receptor (FXR aka NR1H4) were up-regulated, whereas the liver X receptor (LXR aka NR1H3) was down-regulated. Another relevant action of geraniol concerns lipid trafficking in blood, as most genes involved in reverse cholesterol transport and lipoprotein metabolism have had their transcription modified under the influence of that monoterpene. Fig. 9 shows the model we propose for the overall effects of geraniol, as suggested from the results obtained in the present work, in our previous studies (Crespo et al., 2013; Galle et al., 2014), and from the literature (Goto et al., 2011; Jun et al., 2014; Takahashi et al., 2002).

In this model, high levels of both the cholesterol and the TGs in serum along with the presence of oxidized LDL—it accelerating atherogenesis—increase the risk of coronary disease (Chung et al., 2008). Because of the action of geraniol in lowering the levels of both of these compounds selectively in the serum compartment, we propose that geraniol—a natural compound having such pronounced hypolipidemic effects—could well constitute an effective prophylactic or therapeutic agent for the prevention and/or treatment of cardiovascular disease.

5. Conclusions

In the present work we have demonstrated that mice administered geraniol

had significantly lower levels of serum cholesterol and TG. The following mechanisms may have mediated this effect: First, a down-regulation of hepatocyte-cholesterol synthesis occurred as a result of decreased HMGCR protein levels and catalytic activity. Second, the levels of LDLR mRNA became elevated, thus suggesting an increase in the uptake of serum LDL, especially by the liver. Three, TG synthesis became reduced very likely because of a decrease in fatty-acid synthesis.

Dietary phytochemicals may alter gene expression in different ways. The results from these experiments provide information on the effects of geraniol on the metabolism of specific lipids that should contribute to a decrease in the risk of cardiovascular disease. To our knowledge, this investigation is one of the first studies demonstrating that geraniol could constitute a potential prophylactic and/or therapeutic agent by lowering both the cholesterol and the TG in serum so as to contribute to a primary as well as a secondary prevention of coronary disease.

Acknowledgements

This work was supported by research grants from Consejo Nacional de Investigaciones Científicas y Técnicas (CONICET) Argentina, Agencia Nacional de Promoción Científica y Tecnológica ANPCyT), and Universidad Nacional de La Plata.

We would like to thank Dr. Donald F.Haggerty, a retired career investigator and native English speaker, for editing the final version of the manuscript.

Conflict of interest

We have no conflicts of interest to declare.

Table legends

Table 1 *Real-time–RT-PCR–primer sequences*

Gene	Primer	Sequence (5´-3´)
HMGCR	Forward	TGTCCTTGATGGCAGCCTTG
	Reverse	CGCGCTTCAGTTCAGTGTCAG
LDLR	Forward	GCAGTAGCTCGCTCTCGTTG
	Reverse	TGGCAATGGATCCCGGAAAG
SREBF2	Forward	AAGGCTGGCCCATAGCTTC
	Reverse	GCAGTAGCTCGCTCTCGTTG
VLDLR	Forward	AGCGCTTCTGTAGGACACAC
	Reverse	CTTCAGCGCTGGCTCTGTTA
ACACA	Forward	GACAGAGGAAGATGGCGTCC
	Reverse	AGATGTGCTGGGTCATGTGG
ß-actin	Forward	TCAAGATCATTGCTCCTCCTGAG
	Reverse	CTCCTGCTTGCTGATCCACA

Table 2 *Effect of geraniol in body and liver weight and in the food intake of mice during a 3-week experimental period.* After that exposure to G (at 0, 25, 50, and 75 mmol G/kg food) body weight (BW), liver weight (LW), food intake, and geraniol intake were measured in the treated and control mice. Values are the means ± SEM (n = 5). Values in a row with similar superscript letters do not differ significantly ($p > 0.05$).

	Control	mmol G/Kg chow		
		25	50	75
Initial BW (g)	20.5 ± 0.4[a]	20.6 ± 0.2[a]	21.0 ± 0.4[a]	20.8 ±0.4[a]
Final BW(g)	25.0± 0.5[a]	24.0±0.5[a]	24.5 ±0.2[a]	24.1 ±0.4 [a]
LW(g)	1.60±0.07[a]	1.56±0,06[a]	1.60±0,05[a]	1.52±0.06[a]
LW / BW	0.064 ±0.002[a]	0.065±0.002[a]	0.065±0.002[a]	0.063±0.002[a]
Food intake (g/day)	4.10 ± 0.26[a]	3.96 ± 0.26[a]	4.02±0.25[a]	3.88±0.23[a]

Figure legends

Fig. 1. *Effect of geraniol on serum cholesterol and triglycerides.* After three weeks of treatment with geraniol (0, 25, 50, and 75 mmol/kg chow) or simvastatin (50mg/kg), serum samples were collected and serum cholesterol and triglycerides measured as described in Materials and Methods. The values represent the means ± SEM, $5 \leq n \leq 8$. (*) $p < 0.05$, (**) $p < 0.01$ *vs*. control group; (##) $p < 0.01$ *vs*. group treated with 25 mmol G/kg chow

Fig. 2. *Histological appearance of livers from mice treated with geraniol.* NIH *nu/nu* mice received either standard chow alone (controls; panels A and C) or supplemented with geraniol (50 mmol/kg chow; panels B and C) for three weeks. Original magnification: 10X (Panels A and B) and 40X (panels C and D); Slices of 6-µm thickness were stained with hematoxylin and eosin.

Fig. 3. *Effect of geraniol on hepatic-lipid content.* Liver lipids were extracted and separated by thin-layer chromatography and the spots visualized with $FeCl_3.H_2SO_4$ (Panel A). The relative quantities of free cholesterol (FC), esterified cholesterol (EC), and triglycerides (TG) were quantified by measuring the intensity of each band (Panel B). The results are expressed as means ± SEM, n = 5.

Fig. 4. *Incorporation of [^{14}C] acetate into the liver lipids of mice fed geraniol.* The radioactivity incorporated into total liver lipids (TL), nonsaponifiable lipids (NL), and fatty acids (FA) was measured by liquid-scintillation counting. The data are the means ± SEM, n = 5. (*) $p < 0.05$, (**) $p < 0.01$, (***) $p < 0.001$.

Fig. 5. In-silico *analysis, in triplicate, of the mRNA-expression profile of lipid-associated genes in the PC-3 cell line.* PC-3 cells were exposed to geraniol or only

to the vehicle (a working solution of 0.01% [v/v] ethanol) as a control. Panel A. Unsupervised hierarchical clustering clearly defined two groups of samples, which distinction indicated that geraniol exerted its effect on gene expression. Moreover, from the first node of the gene tree, two groups were identified: the upper cluster (designated *down-regulated*) with genes whose expression decreased upon treatment with geraniol and the lower cluster (designated *up-regulated*) with genes whose expression increased upon treatment with geraniol. The figure also indicates how the biologic processes associated with these genes were likewise distributed according to the hierarchical clustering. Panel B. To determine whether these differences were significant, a TTest analysis and subsequent hierarchical clustering of the significant genes was conducted. Out of 64 genes, 30 showed statistical differences ($p < 0.05$). We then decided to validate in our mouse model five of those genes (indicated by the red and green arrows), of which the figure shows box-whisker plots of their expression profile in the PC-3 cells.Genes are named with the official symbol according to HGNC (HUGO Gene Nomenclature Committee)

Fig. 6. *HMGCR in mice treated with geraniol.* The mRNA levels of liver HMGCR were determined by real-time RT-PCR (Panel A), while the quantity of enzyme protein was measured by Western blotting (Panel B). Under this graph are also shown the Western-blot densities of immunoreactive HMGCR protein (above) and the polyvinylidenedifluoride (PVDC) staining with Coomassie brilliant blue G-250 (below). Finally, the enzyme's catalytic activity was assayed in liver microsomes (Panel C). The results are expressed as the means ± SEM, n = 4. (*) $p < 0.05$, (**) $p < 0.01$ *vs*. control group, (#) $p < 0.05$ *vs*. the group treated with 25 mmol G/kg of diet.

Fig. 7. *Expression of LDL-receptor– and SREBF-2–mRNA transcription in mice fed geraniol.* The mRNA was obtained from the livers of mice after three weeks of treatment as described in Materials and Methods and the relative amount (with

respect to ß-actin) of LDL receptor- (Panel A) and SREBF2- (Panel B) mRNA determined. The results are expressed as the means ± SEM, with n = 4, (*) $p < 0.05$ *vs*. the control group.

Fig. 8. *The effect of geraniol on ACACA- and VLDL-receptor–mRNA transcription.* mRNA was obtained from the mouse livers and the relative amount (with respect to ß-actin) of ACACA- (Panel A) and VLDL receptor- (Panel B) mRNA determined. The results are expressed as the means ± SEM, with n = 4, (*) $p < 0.05$ *vs*. the control group.

Fig. 9. *Proposed model for the effects of geraniol.* The geraniol mechanisms of action proposed are represented in this panel. The Kyoto Encyclopedia of Genes and Genomes (Kegg) symbols were used representing gene expression (→O→), gene repression (→IO→), transcriptional or post-transcriptional gene repression (-----|) protein activation (→) and protein inhibition (–|). The genes up-regulated in the *in silico* analysis are in red and those down-regulated in green.Genes are named with the official symbol according to HGNC (HUGO Gene Nomenclature Committee). TG: Triglycerides; FA: fatty acids.

References

Ahmad, S.T., Arjumand, W., Seth, A., Nafees, S., Rashid, S., Ali, N., Sultana, S., 2011. Preclinical renal cancer chemopreventive efficacy of geraniol by modulation of multiple molecular pathways. Tox 290, 69-81.

Bradford, M.M., 1976. A rapid and sensitive method for the quantitation of microgram quantities of protein utilizing the principle of protein-dye binding. Anal Biochem 72, 248-254.

Burke, Y.D., Stark, M.J., Roach, S.L., Sen, S.E., Crowell, P.L., 1997. Inhibition of pancreatic cancer growth by the dietary isoprenoids farnesol and geraniol. Lipids 32, 151-156.

Cardozo, M.T., de Conti, A., Ong, T.P., Scolastici, C., Purgatto, E., Horst, M.A., Bassoli, B.K., Moreno, F.S., 2011. Chemopreventive effects of beta-ionone and geraniol during rat hepatocarcinogenesis promotion: distinct actions on cell proliferation, apoptosis, HMGCoA reductase, and RhoA. J Nutr Biochem 22, 130-135.

Carnesecchi, S., Schneider, Y., Ceraline, J., Duranton, B., Gosse, F., Seiler, N., Raul, F., 2001. Geraniol, a component of plant essential oils, inhibits growth and polyamine biosynthesis in human colon cancer cells. J Pharmacol Exp Ther 298, 197-200.

Crawford, D.C., Nord, A.S., Badzioch, M.D., Ranchalis, J., McKinstry, L.A., Ahearn, M., Bertucci, C., Shephard, C., Wong, M., Rieder, M.J., Schellenberg, G.D., Nickerson, D.A., Heagerty, P.J., Wijsman, E.M., Jarvik, G.P., 2008. A common VLDLR

polymorphism interacts with APOE genotype in the prediction of carotid artery disease risk. J Lipid Res 49, 588-596.

Crespo, R., Montero Villegas, S., Abba, M.C., de Bravo, M.G., Polo, M.P., 2013. Transcriptional and posttranscriptional inhibition of HMGCR and PC biosynthesis by geraniol in 2 Hep-G2 cell proliferation linked pathways. Biochem Cell Biol 91, 131-139.

Chang, T.Y., Chang, C.C., Ohgami, N., Yamauchi, Y., 2006. Cholesterol sensing, trafficking, and esterification. Annu Rev Cell Dev Biol 22, 129-157.

Chaudhary, S.C., Siddiqui, M.S., Athar, M., Alam, M.S., 2013. Geraniol inhibits murine skin tumorigenesis by modulating COX-2 expression, Ras-ERK1/2 signaling pathway and apoptosis. J Appl Toxicol 33, 828-837.

Chen, W., Viljoen, A.M., 2010. Geraniol—A review of a commercially important fragrance material. S. Afr. J. Bot. 76, 643-651.

Chung, M.J., Park, K.W., Kim, K.H., Kim, C.T., Baek, J.P., Bang, K.H., Choi, Y.M., Lee, S.J., 2008. Asian plantain (Plantago asiatica) essential oils suppress 3-hydroxy-3-methyl-glutaryl-co-enzyme A reductase expression in vitro and in vivo and show hypocholesterolaemic properties in mice. Br J Nutr 99, 67-75.

Dudley, R.A., Anderson, R.E., 1975. Separation of polyunsaturated fatty acids by argentation thin layer chromatography. Lipids 10, 113-115.

Dudoit, S., Yang, Y.H., Callow, M.J., Speed, T.P., 2002. Statistical methods for identifying differentially expressed genes in replicated cDNA microarray experiments. Stat sin 12, 111-140.

Duncan, R.E., Lau, D., El-Sohemy, A., Archer, M.C., 2004. Geraniol and beta-ionone inhibit proliferation, cell cycle progression, and cyclin-dependent kinase 2 activity in MCF-7 breast cancer cells independent of effects on HMG-CoA reductase activity. Biochem Pharmacol 68, 1739-1747.

Espenshade, P.J., Hughes, A.L., 2007. Regulation of sterol synthesis in eukaryotes. Annu Rev Genet 41, 401-427.

Folch, J., Lees, M., Sloane Stanley, G.H., 1957. A simple method for the isolation and purification of total lipides from animal tissues. J Biol Chem 226, 497-509.

Galle, M., Crespo, R., Rodenak Kladniew, B., Montero Villegas, S., Polo, M., de Bravo, M.G., 2014. Suppression by geraniol of the growth of a549 human lung adenocarcinoma cells and inhibition of the mevalonate pathway in culture and in vivo: potential use in cancer chemotherapy. Nutr cancer 66, 888-895.

Goldstein, J.L., Brown, M.S., 1990. Regulation of the mevalonate pathway. Nature 343, 425-430.

Goto, T., Kim, Y.I., Funakoshi, K., Teraminami, A., Uemura, T., Hirai, S., Lee, J.Y., Makishima, M., Nakata, R., Inoue, H., Senju, H., Matsunaga, M., Horio, F., Takahashi, N., Kawada, T., 2011. Farnesol, an isoprenoid, improves metabolic abnormalities in mice via both PPARalpha-dependent and -independent pathways. Am J Physiol Endocrinol Metab 301, E1022-1032.

Guo-Min, S., Ying-Ze, Z., Ming-Tai, C., Feng-Lin, Z., Xiao-Ling, L., Yi, W., ..., & Jun-Wu, Z., 2012. Hypoxia-inducible factor-1 (HIF-1)

promotes LDL and VLDL uptake through inducing VLDLR under hypoxia. Biochem J 441, 675-683.

Jayachandran, M., Chandrasekaran, B., Namasivayam, N., 2014. Effect of geraniol, a plant derived monoterpene on lipids and lipid metabolizing enzymes in experimental hyperlipidemic hamsters. Mol Cell Biochem 398(1-2), 39-53.

Jin, X., Sun, J., Miao, X., Liu, G., Zhong, D., 2013. Inhibitory effect of geraniol in combination with gemcitabine on proliferation of BXPC-3 human pancreatic cancer cells. Journal int med res 41, 993-1001.

Jun, H.J., Lee, J.H., Kim, J., Jia, Y., Kim, K.H., Hwang, K.Y., Yun, E.J., Do, K.R., Lee, S.J., 2014. Linalool is a PPARalpha ligand that reduces plasma TG levels and rewires the hepatic transcriptome and plasma metabolome. J Lipid Res 55, 1098-1110.

Kim, S.H., Park, E.J., Lee, C.R., Chun, J.N., Cho, N.H., Kim, I.G., Lee, S., Kim, T.W., Park, H.H., So, I., Jeon, J.H., 2012. Geraniol induces cooperative interaction of apoptosis and autophagy to elicit cell death in PC-3 prostate cancer cells. Int J Oncol 40, 1683-1690.

Lapczynski, A., Bhatia, S.P., Foxenberg, R.J., Letizia, C.S., Api, A.M., 2008. Fragrance material review on geraniol. Food Chem Toxicol 46 Suppl 11, S160-170.

Lee, S., Chun, J.N., Kim, S.H., So, I., Jeon, J.H., 2013. Icilin inhibits E2F1-mediated cell cycle regulatory programs in prostate cancer. Biochem Biophys Res Commun 441, 1005-1010.

Li, Y.C., Park, M.J., Ye, S.K., Kim, C.W., Kim, Y.N., 2006. Elevated levels of cholesterol-rich lipid rafts in cancer cells are correlated with

apoptosis sensitivity induced by cholesterol-depleting agents. Am J Pathol 168, 1107-1118; quiz 1404-1105.

Llorente, A., van Deurs, B., Sandvig, K., 2007. Cholesterol regulates prostasome release from secretory lysosomes in PC-3 human prostate cancer cells. Eur J Cell Biol 86, 405-415.

Mo, H., Elson, C.E., 2004. Studies of the isoprenoid-mediated inhibition of mevalonate synthesis applied to cancer chemotherapy and chemoprevention. Exp Biol Med 229, 567-585.

Ong, T.P., Heidor, R., de Conti, A., Dagli, M.L., Moreno, F.S., 2006. Farnesol and geraniol chemopreventive activities during the initial phases of hepatocarcinogenesis involve similar actions on cell proliferation and DNA damage, but distinct actions on apoptosis, plasma cholesterol and HMGCoA reductase. Carcinogenesis 27, 1194-1203.

Pan, W., 2002. A comparative review of statistical methods for discovering differentially expressed genes in replicated microarray experiments. Bioinformatics 18, 546-554.

Peffley, D.M., Gayen, A.K., 2003. Plant-derived monoterpenes suppress hamster kidney cell 3-hydroxy-3-methylglutaryl coenzyme a reductase synthesis at the post-transcriptional level. J Nutr 133, 38-44.

Polo, M.P., Crespo, R., de Bravo, M.G., 2011. Geraniol and simvastatin show a synergistic effect on a human hepatocarcinoma cell line. Cell Biochem Funct 29, 452-458.

Polo, M.P., de Bravo, M.G., 2006. Effect of geraniol on fatty-acid and mevalonate metabolism in the human hepatoma cell line Hep G2. Biochem Cell Biol 84, 102-111.

Ren, Z., Gould, M.N., 1994. Inhibition of ubiquinone and cholesterol synthesis by the monoterpene perillyl alcohol. Cancer Lett 76, 185-190.

Sato, R., 2009. SREBPs: protein interaction and SREBPs. The FEBS journal 276, 622-627.

Tacken, P.J., Teusink, B., Jong, M.C., Harats, D., Havekes, L.M., van Dijk, K.W., Hofker, M.H., 2000. LDL receptor deficiency unmasks altered VLDL triglyceride metabolism in VLDL receptor transgenic and knockout mice. J Lipid Res 41, 2055-2062.

Takahashi, N., Kawada, T., Goto, T., Yamamoto, T., Taimatsu, A., Matsui, N., Kimura, K., Saito, M., Hosokawa, M., Miyashita, K., Fushiki, T., 2002. Dual action of isoprenols from herbal medicines on both PPARgamma and PPARalpha in 3T3-L1 adipocytes and HepG2 hepatocytes. FEBS Lett 514, 315-322.

Vallianou, I., Peroulis, N., Pantazis, P., Hadzopoulou-Cladaras, M., 2011. Camphene, a plant-derived monoterpene, reduces plasma cholesterol and triglycerides in hyperlipidemic rats independently of HMG-CoA reductase activity. PLoS One 6, e20516.

van der Wulp, M.Y., Verkade, H.J., Groen, A.K., 2013. Regulation of cholesterol homeostasis. Mol Cell Endocrinol 368, 1-16.

Wang, J., Zhou, G., Chen, C., Yu, H., Wang, T., Ma, Y., Jia, G., Gao, Y., Li, B., Sun, J., Li, Y., Jiao, F., Zhao, Y., Chai, Z., 2007. Acute toxicity

and biodistribution of different sized titanium dioxide particles in mice after oral administration. Toxicol Lett 168, 176-185.

Wilson, R., Sargent, J.R., 1992. High-resolution separation of polyunsaturated fatty acids by argentation thin-layer chromatography. J Chromatogr A 623, 403-407.

Wiseman, D.A., Werner, S.R., Crowell, P.L., 2007. Cell cycle arrest by the isoprenoids perillyl alcohol, geraniol, and farnesol is mediated by p21(Cip1) and p27(Kip1) in human pancreatic adenocarcinoma cells. J Pharmacol Exp Ther 320, 1163-1170.

Wolfensohn, S., and Lloyd M.; 2013. Handbook of Laboratory Animal Management and Welfare, 4th Edition,John Wiley & Sons, Oxford, Wiley-Blackwell,.

Yu, S. G., Hildebrandt, L. A., and Elson, C. E., 1995. Geraniol, an inhibitor of mevalonate biosynthesis, suppresses the growth of hepatomas and melanomas transplanted to rats and mice. J Nutr 25(11), 2763-2767.

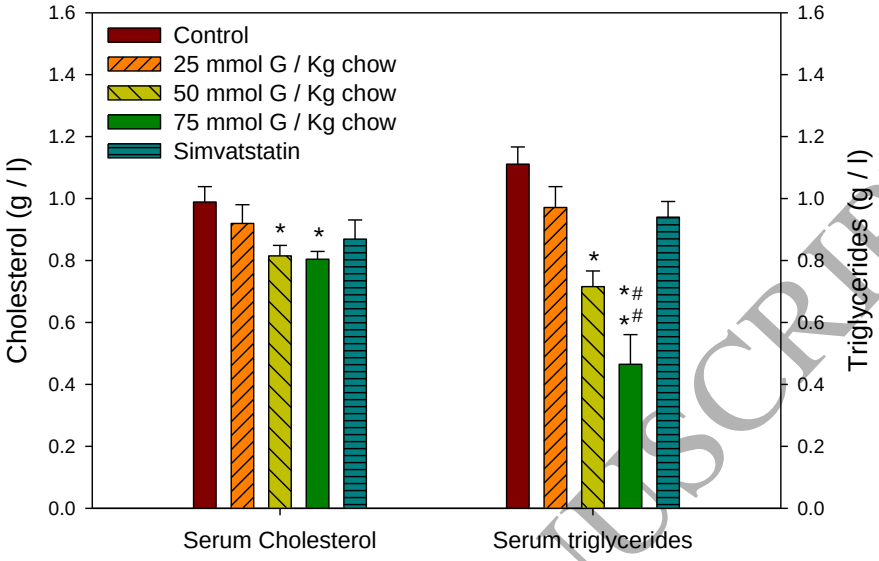

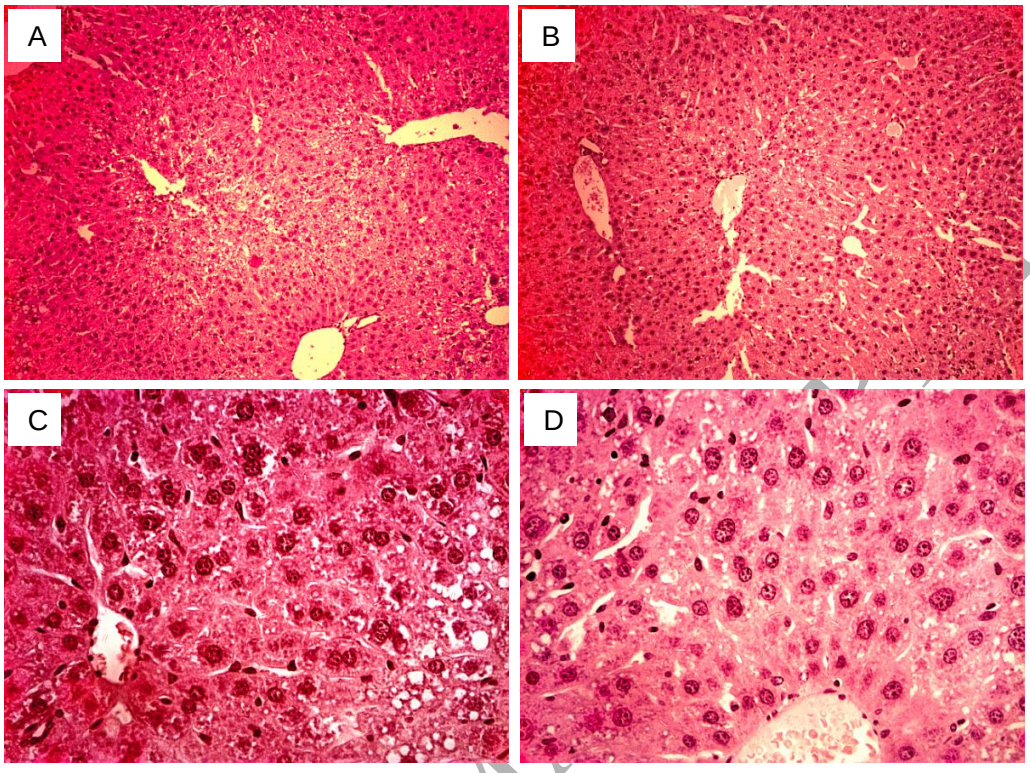

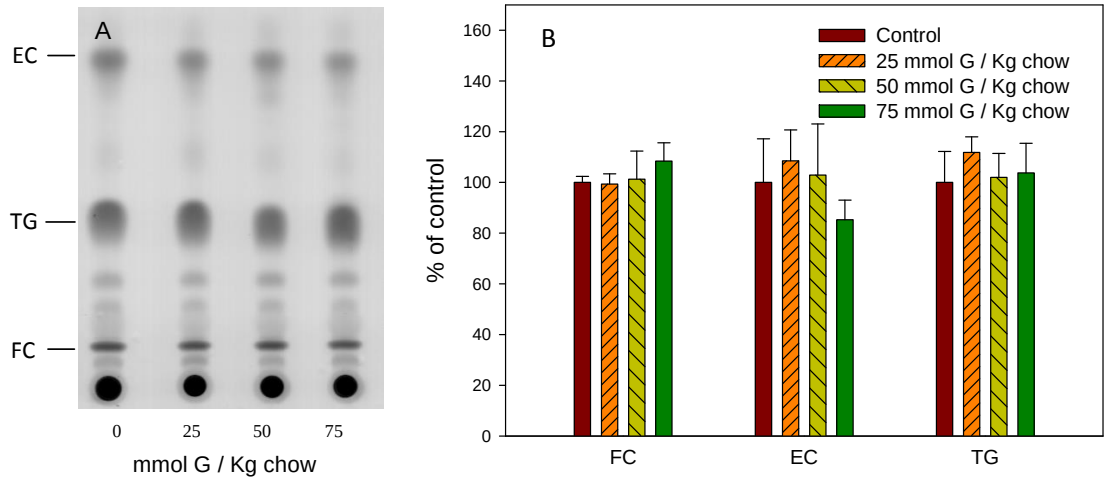

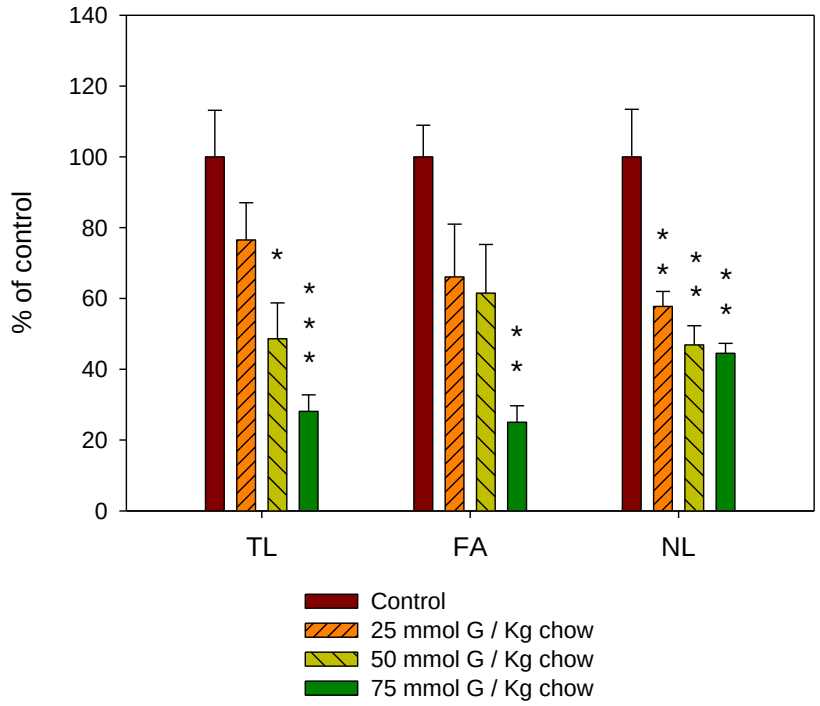

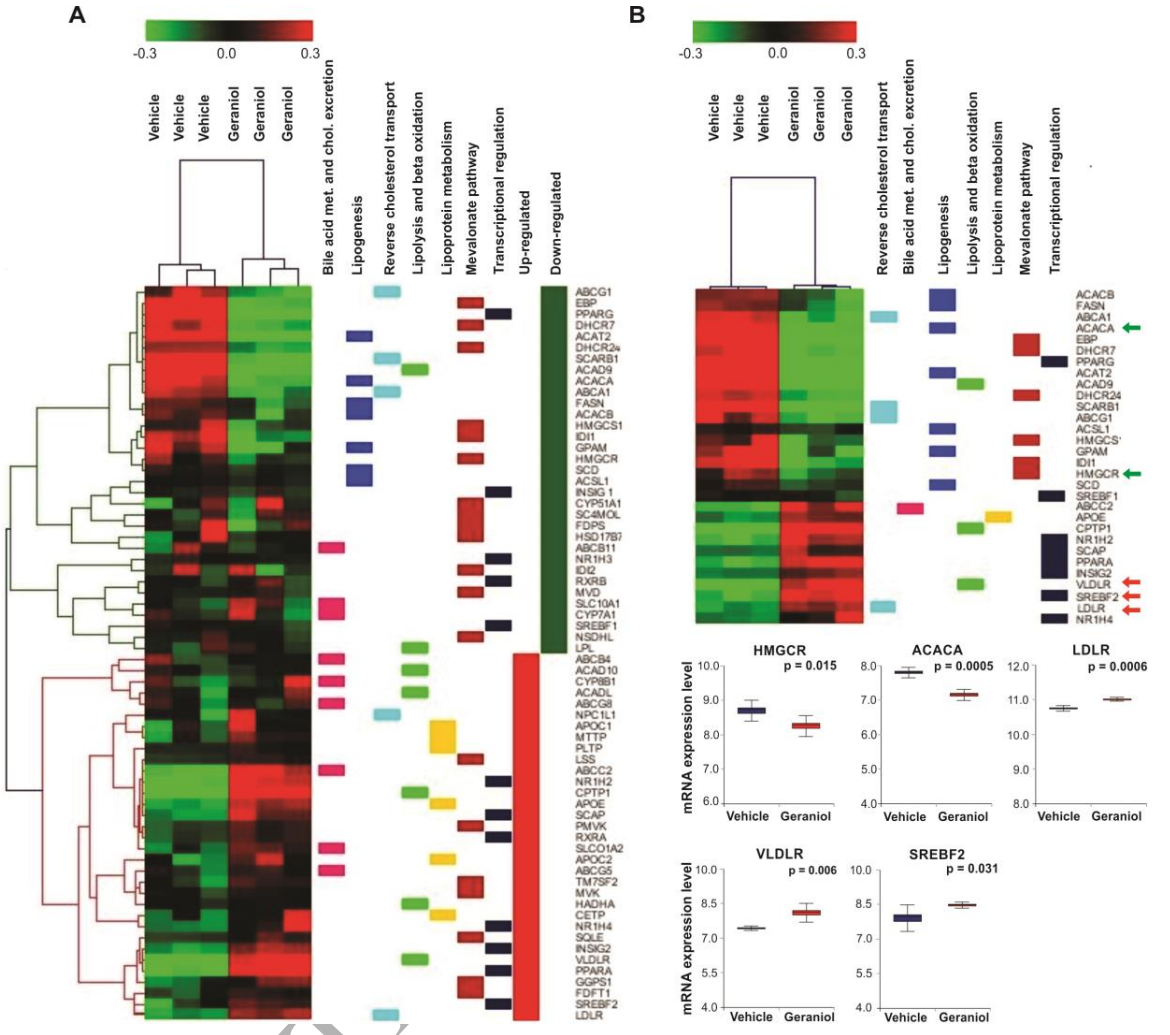
A
-0.3
0.0
0.3
Vehicle
Vehicle
Vehicle
Geraniol
Geraniol
Geraniol
Bile acid met. and chol. excretion
Lipogenesis
Reverse cholesterol transport
Lipolysis and beta oxidation
Lipoprotein metabolism
Mevalonate pathway
Transcriptional regulation
Up-regulated
Down-regulated
ABCG1
EBP
PPARG
DHCR7
ACAT2
DHCR24
SCARB1
ACAD9
ACACA
ABCA1
FASN
ACACB
HMGCS1
IDI1
GPAM
HMGCR
SCD
ACSL1
INSIG 1
CYP51A1
SC4MOL
FDPS
HSD17B7
ABCB11
NR1H3
IDI2
RXRB
MVD
SLC10A1
CYP7A1
SREBF1
NSDHL
LPL
ABCB4
ACAD10
CYP8B1
ACADL
ABCG8
NPC1L1
APOC1
MTTP
PLTP
LSS
ABCC2
NR1H2
CPTP1
APOE
SCAP
PMVK
RXRA
SLCO1A2
APOC2
ABCG5
TM7SF2
MVK
HADHA
CETP
NR1H4
SQLE
INSIG2
VLDLR
PPARA
GGPS1
FDFT1
SREBF2
LDLR
B
-0.3
0.0
0.3
Vehicle
Vehicle
Vehicle
Geraniol
Geraniol
Geraniol
Reverse cholesterol transport
Bile acid met. and chol. excretion
Lipogenesis
Lipolysis and beta oxidation
Lipoprotein metabolism
Mevalonate pathway
Transcriptional regulation
ACACB
FASN
ABCA1
ACACA
EBP
DHCR7
PPARG
ACAT2
ACAD9
DHCR24
SCARB1
ABCG1
ACSL1
HMGCS1
GPAM
IDI1
HMGCR
SCD
SREBF1
ABCC2
APOE
CPTP1
NR1H2
SCAP
PPARA
INSIG2
VLDLR
SREBF2
LDLR
NR1H4
HMGCR
p = 0.015
ACACA
p = 0.0005
LDLR
p = 0.0006
mRNA expression level
Vehicle
Geraniol
VLDLR
p = 0.006
SREBF2
p = 0.031

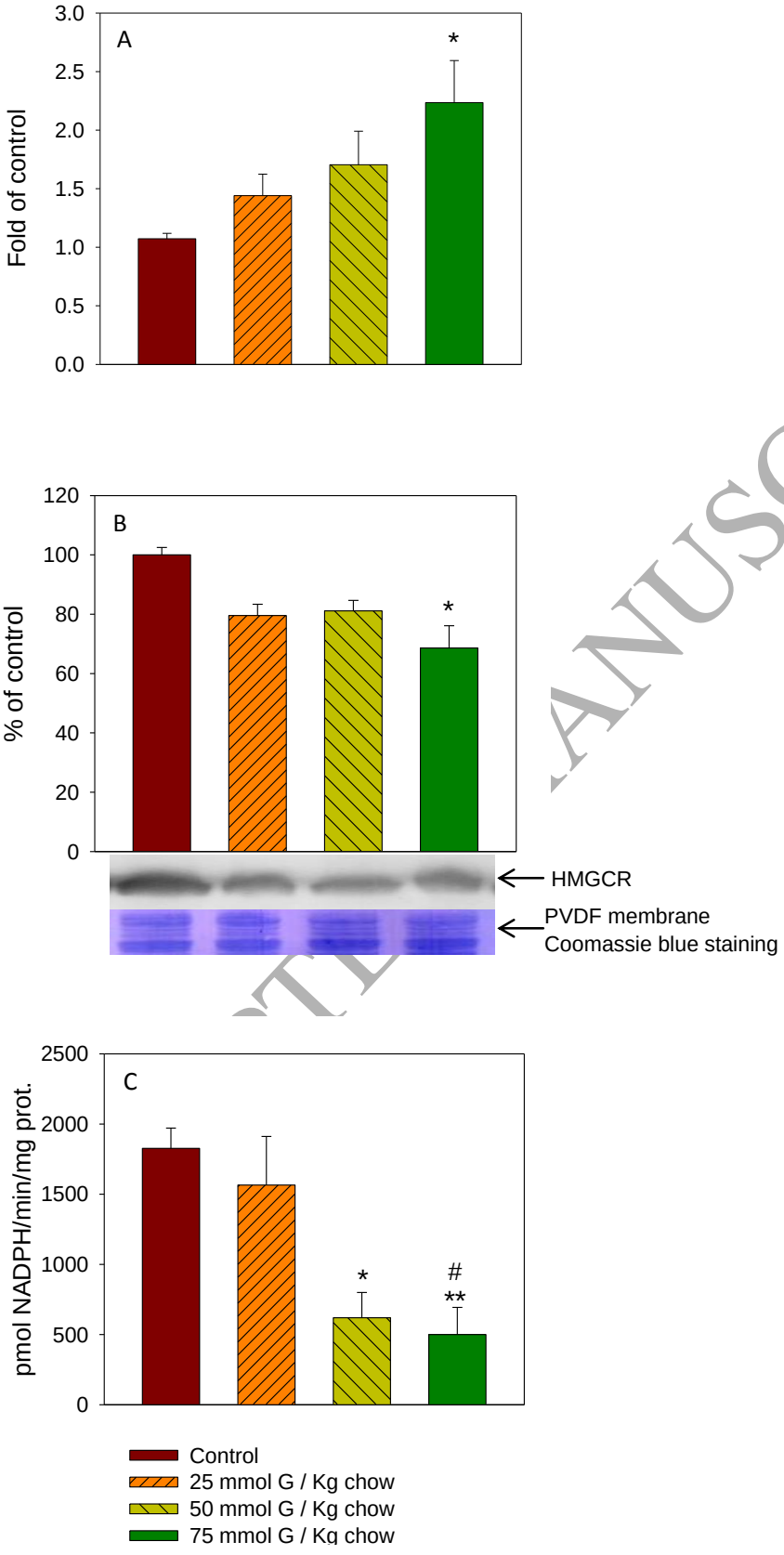

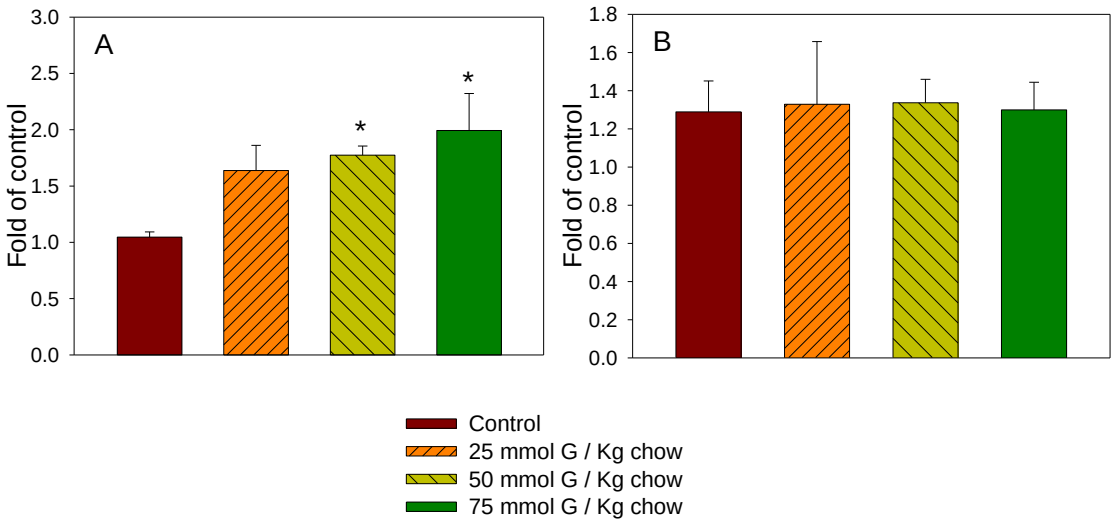

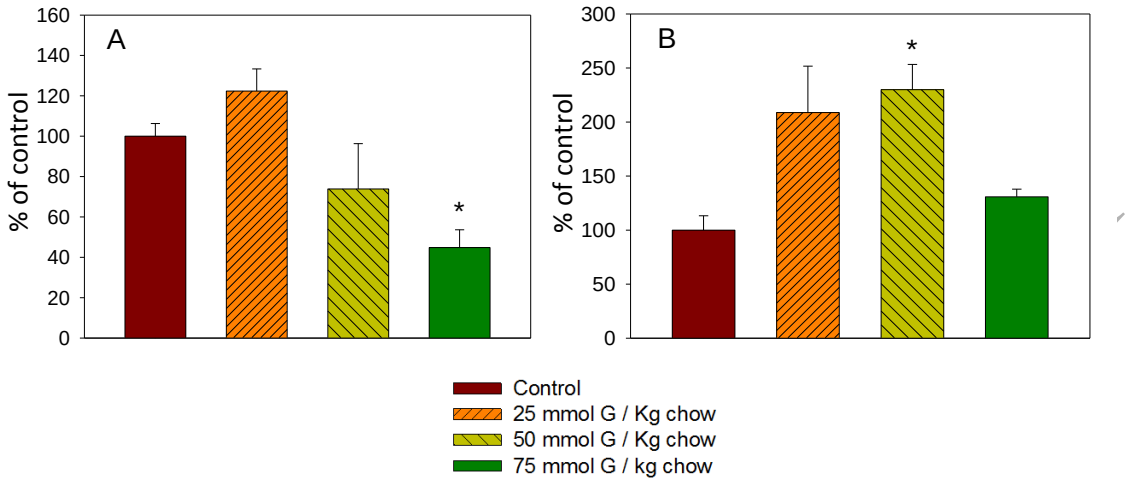

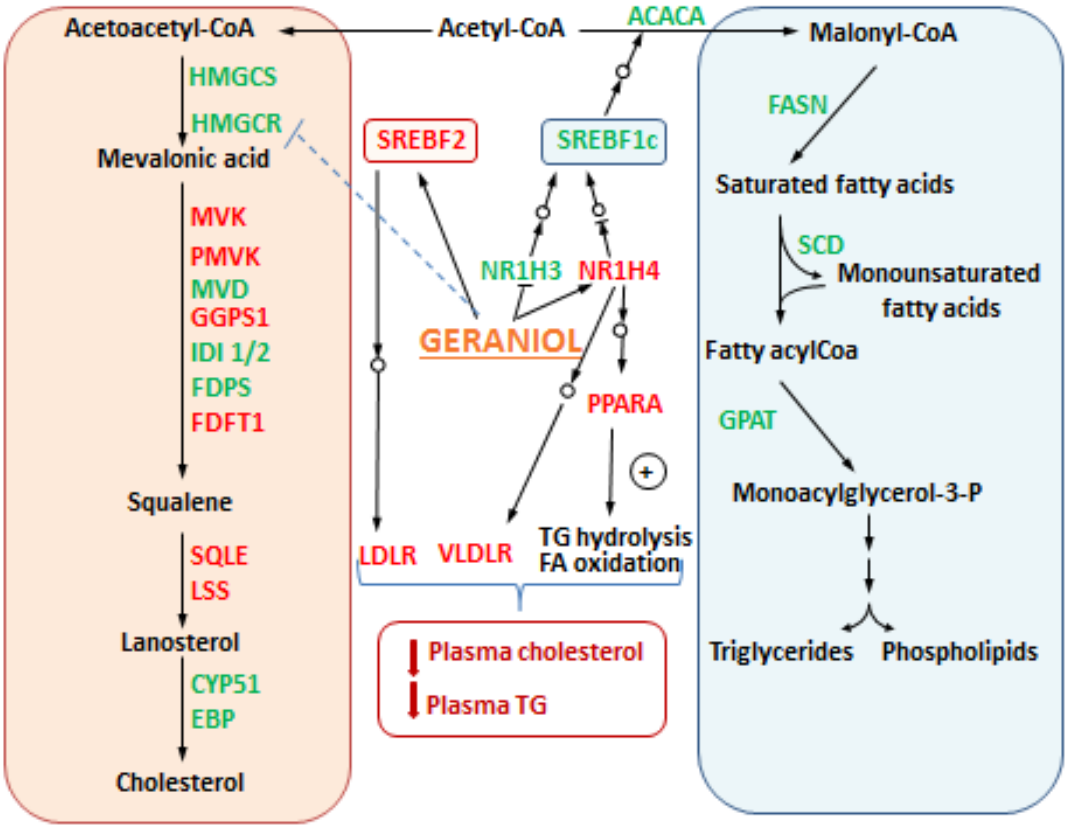
Acetoacetyl-CoA
Acetyl-CoA
ACACA
Malonyl-CoA
HMGCS
HMGCR
Mevalonic acid
MVK
PMVK
MVD
GGPS1
IDI 1/2
FDPS
FDFT1
Squalene
SQLE
LSS
Lanosterol
CYP51
EBP
Cholesterol
SREBF2
SREBF1c
NR1H3
NR1H4
GERANIOL
PPARA
LDLR
VLDLR
TG hydrolysis
FA oxidation
Plasma cholesterol
Plasma TG
FASN
Saturated fatty acids
SCD
Monounsaturated
fatty acids
Fatty acylCoa
GPAT
Monoacylglycerol-3-P
Triglycerides
Phospholipids